FUNCTIONAL GROUP AND MOLECULAR STRUCTURE PRODUCE SOLVATION STRUCTURE: RAMAN SPECTROSCOPY AND THEORETICAL ANALISIS

D. Kajiya[1] and K. Saitow[1, 2, *]

[1]*Natural Science Center for Basic Research and Development (N-BARD), Hiroshima University, 1-3-1 Kagamiyama, Higashi-hiroshima, Hiroshima 739-8526, Japan*
[2]*Department of Chemistry, Graduate School of Science, Hiroshima University, 1-3-1 Kagamiyama, Higashi-hiroshima, Hiroshima 739-8526, Japan*
* Corresponding author: Telephone & fax: +81-82-424-7487, e-mail: saitow@hiroshima-u.ac.jp

ABSTRACT

The vibrational Raman spectra of the C=C stretching modes of *cis*-dichloroethylene (*cis*-DCE), *cis*-diphenylethylene (*cis*-DPE), and *trans*-diphenylethylene (*trans*-DPE) were measured in supercritical carbon dioxide (scCO$_2$) and supercritical fluoroform (scCHF$_3$) an isotherm of $T_r = T/T_c = 1.02$ over wide range of density. As the density increased, peak frequencies of the C=C stretching modes shifted toward the low-energy side. The shifted amount of *trans*-DPE was 20 times greater than that of *cis*-DCE. This enormous shift of *trans*-DPE was caused by significant attractive energy between solute and solvent molecules owning to a functional group effect of phenyl group in the absence of steric hindrance.

INTRODUCTION

Vibrational motions of a molecule in a fluid are perturbed by continuous intermolecular interactions of surrounding molecules [1–3]. As a density of fluid increases from isolated condition, vibrational spectrum of a molecule shifts toward lower or higher energy. The shifted amount depends on the magnitudes of attractive and repulsive energies among molecules [4–17]. By using neat supercritical fluids and supercritical solutions, vibrational Raman and/or infrared spectroscopic studies have been performed over wide range of densities. On the basis of intermolecular interactions, these supercritical systems are classified into three groups: Group I: systems involving hydrogen bonding [18–20]; Group II: systems involving strong dipole–dipole

1

interactions [8,20,21]; and Group III: systems involving the formation of complexes between solute and solvent molecules [9].

In our previous studies, we have investigated supercritical fluid structures by means of dynamic light scattering [22–25], terahertz absorption [26,27], vibrational Raman spectroscopy [7,8,10,13–16,28–30], and nanoparticle generation [31–34]. In the Raman spectroscopic studies, the attractive and repulsive energies between solute and solvent molecules have been evaluated by theoretical analysis of density dependence of Raman spectra. For example, solvation structure around solute molecule is elucidated by 3D schematic diagram [15].

In the present study, we show that functional group and molecular structure of solute molecule produce solvation structure in supercritical solutions. We measured vibrational Raman spectra of C=C stretching modes of three kinds of ethylene derivatives (Fig. 1) in supercritical scCO$_2$ and scCHF$_3$. As a result, enormous frequency shift was observed in *trans*-DPE. The magnitude of the shift was equivalent to those of typical hydrogen-bonded fluids, and can be categorized as new type of system, i.e., Group IV. Such a significant shift was attributed to functional group effect of phenyl groups in the absence of steric hindrance.
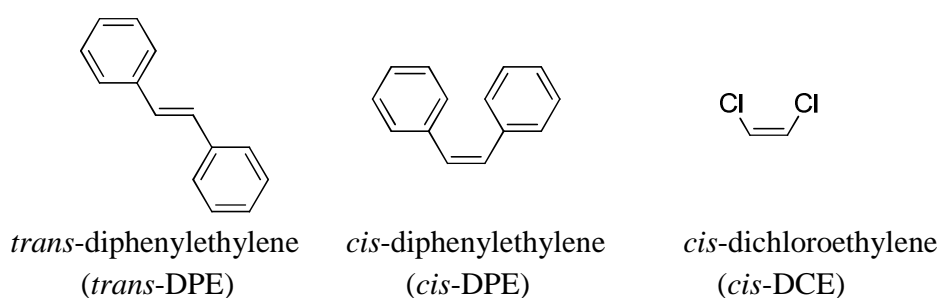

trans-diphenylethylene   *cis*-diphenylethylene   *cis*-dichloroethylene
(*trans*-DPE)   (*cis*-DPE)   (*cis*-DCE)

Figure 1. Molecular structures of solute molecules.

EXPERIMENTAL SECTION

Raman spectra were measured with an instrument developed in our lab and described elsewhere [10,13]. The light source was a diode-pumped solid-state laser operated with an excitation wavelength of 532 nm, at a single frequency output of 200 mW, in front of an optical cell. The laser was incident on the cell and a camera lens collected the scattered light at an angle of 90° relative to incident line. Using a monochromator and a photomultiplier tube, Raman spectra were recorded using the photon counting method. The frequency of each Raman spectrum was calibrated by that of the exciting laser. The frequency repeatability was confirmed to be within ±0.02 cm^{-1}. The high-frequency stability enabled very precise peak position measurements in the Raman spectra.

Supercritical solutions of Raman spectral measurements were prepared as follows: An accurate volume of solute molecule was introduced into a high-pressure container. The container was then filled with high-pressure CO_2 or CHF_3 by measuring the weight of the container during fluid injection. The high-pressure solution generated in the container was then transferred into a Raman optical cell. The densities of the supercritical solutions were adjusted by releasing the high-pressure supercritical solution from the Raman cell. The temperature was maintained along an isotherm of reduced temperature $T_r = T/T_c = 1.02$, by using a set up comprising of a proportional–integral–derivative controller, heaters, and a thermocouple. The pressure was monitored using a strain gauge backed up with a strain amplifier. Both temperature and pressure fluctuations were within the range of ±0.1% during the measurements. Densities were calculated from the empirical state equation by using P and T values [35,36], and were varied in the range of $0.08 < \rho_r < 1.7$, where the ρ_r is the reduced density represented by $\rho_r = \rho/\rho_c$. The critical constants of CO_2 and CHF_3 are reported to be $T_c = 304.1$ K, $P_c = 7.4$ MPa, $\rho_c = 0.468$ g cm^{-3} [35] and $T_c = 299.3$ K, $P_c = 4.8$ MPa, $\rho_c = 0.527$ g cm^{-3} [36], respectively.

RESULTS AND DISCUSSION

Fig. 2 shows frequency shifts $\Delta\nu$ of the C=C stretching modes of *trans*-DPE, *cis*-DPE, and *cis*-DCE in scCO$_2$ (Fig. 1a) and scCHF$_3$ (Fig. 1b). The $\Delta\nu$ is obtained by $\Delta\nu = \nu - \nu_0$, where ν and ν_0 are the experimental peak frequencies and that of density = 0, respectively. As the density increases, the $\Delta\nu$ increases in all supercritical solutions. Note that $\Delta\nu$ of *trans*-DPE shows twice greater than that of *cis*-DPE and 20 times greater than that of *cis*-DCE. The $\Delta\nu$ of *trans*-DPE is so large among 50 systems for vibrational spectroscopic studies on supercritical fluids and is equivalent to those of typical hydrogen-bonded fluids [30].
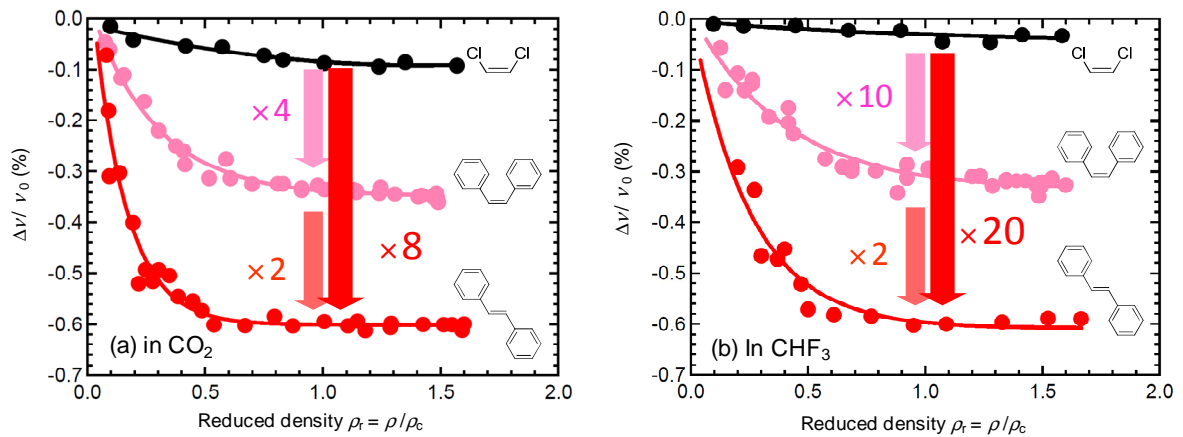

Figure 2. Frequency shifts of C=C stretching modes of *trans*-DPE (red), *cis*-DPE (pink), and *cis*-C$_2$H$_2$Cl$_2$ (black) in scCO$_2$ (a) and in scCHF$_3$ (b) at $T_r = 1.02$. Solid lines are visual guides by fitting polynomial functions. The quantity of ρ_r is expressed as $\rho_r = \rho/\rho_c$.

To discuss such a large frequency shift of *trans*-DPE in supercritical fluids, we analyzed the magnitude of the shifts by considering attractive and repulsive components using the perturbed hard-sphere theory [37]:

$$\Delta \nu = \Delta \nu_R + \Delta \nu_A, \tag{1}$$

where $\Delta \nu$, $\Delta \nu_R$, and $\Delta \nu_A$ are the net, repulsive, and attractive frequency shifts, respectively. The $\Delta \nu_A$ was obtained by subtracting the $\Delta \nu_R$ from the $\Delta \nu$. The $\Delta \nu_R$ was obtained from a theoretical calculation. According to the perturbed hard-sphere theory [37], the $\Delta \nu_R$ is expressed as

$$\frac{\Delta \nu_R}{\nu_0} = C_1 \exp\left(m_1 \rho^*\right) + C_2 \exp\left(m_2 \rho^*\right) - C_3 \exp\left(m_3 \rho^*\right), \tag{2}$$

with $C_k = k \alpha_R \theta z (1-z)^{k-1} \exp b_k$ and $\alpha_R = r_e[-(3g/2f) + (G_R/F_R)]$, where m_k and b_k refer to empirical parameters, which depend on the sizes of solute and solvent molecules. The quantity ρ^* is represented by $\rho^* = \rho_S \sigma_S^3$, where ρ_S is the number density and σ_S is the diameter of the solvent hard sphere. The quantity θ is given by $\theta = k_B T / f r_e^2$, where k_B is the Boltzmann constant and r_e is the equilibrium bond length of the C=C bond. The value of z is expressed as $z = r_e/\sigma$ with two hard-sphere cavities of diameter σ. The values f and g are the intramolecular quadratic harmonic and cubic anharmonic force constants of the C=C bond, respectively, and F_R and G_R are the linear and quadratic constants, respectively, indicating the forces that solvent molecules exert along the normal coordinate of the solute. All parameters required for the calculations were described elsewhere [30].

Fig. 3 shows the repulsive and attractive shifts of *trans*-DPE in scCO$_2$. The repulsive shift increases with increasing fluid density, indicating that the increase in the density causes an increase in the repulsive energy for the C=C stretching mode. The attractive shift also increases with increasing solvent density. The energy of the solute–solvent attractive interactions increases
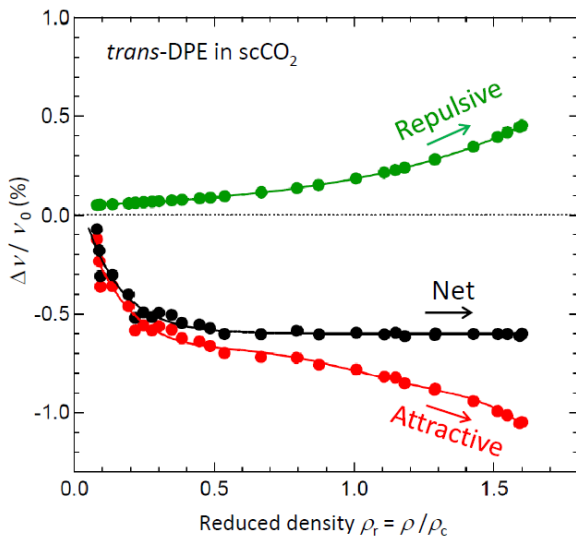

Figure 3 Repulsive (green), net (black), and attractive (red) shifts of C=C stretching modes of *trans*-DPE in scCO$_2$ at T_r = 1.02. Solid lines are visual guides obtained by fitting polynomial functions to the data. The quantity of ρ_r is expressed as $\rho_r = \rho/\rho_c$.

4

with increasing solvent density. Note that the attractive energy is significantly greater than the repulsive energy in all density. Thus, it is found that *trans*-DPE/scCO$_2$ is an attractive mixture.

Fig. 4 shows a comparison of attractive shifts of three ethylene derivatives (*cis*-DPE, *cis*-DCE, and *trans*-DPE) in scCO$_2$. The attractive shift of *cis*-DPE is greater than that of *cis*-DCE. This has been ascribed to a functional group effect of site-selective solvation around the phenyl group of *cis*-DPE [16]. The shift of *trans*-DPE is larger than that of *cis*-DPE. In order to consider the difference of *cis*-DPE and *trans*-DPE, we focused on molecular structures of both isomers. As illustrated in Fig. 4, a *trans*-DPE molecule has two phenyl groups with no steric hindrance. On the other hand, the two phenyl groups of *cis*-DPE exhibit steric hindrance. That is, the two isomers have completely different 3D structures. In *trans*-DPE, there is a space between the two phenyl groups, whereas such a space does not exist in *cis*-DPE. Given this situation, many solvent molecules can surround the two phenyl groups in *trans*-DPE. Molecular dynamics simulations of alkaloids in scCO$_2$ exhibit a similar phenomenon [38]; the steric hindrance of alkaloids obstructs solvation. Present experimental results clearly showed that the steric hindrance yielded a significant difference in attractive energies between solute and solvent molecules.
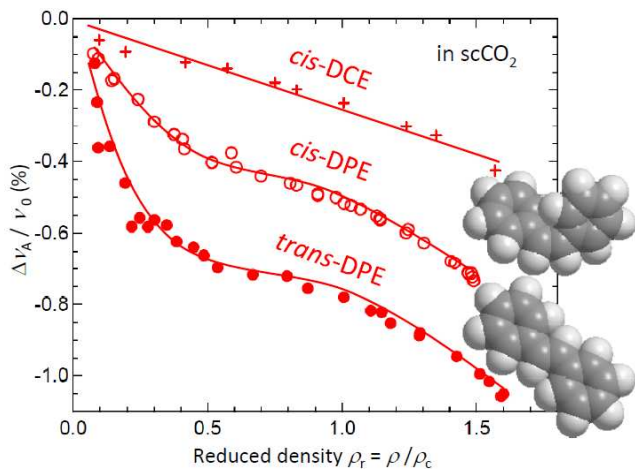

Figure 4 Attractive shift of *trans*-DPE (closed circle), *cis*-DPE (open circle), and *cis*-C$_2$H$_2$Cl$_2$ (+) in scCO$_2$. Solid lines are visual guides obtained by fitting polynomial functions to the data. The quantity of ρ_r is expressed as $\rho_r = \rho/\rho_c$.

In order to further evaluate the steric hindrance effect on solvation structures, we analyze the local density augmentation (LDA) of solvent molecules around *cis*-, and *trans*-DPE. According to the numerous studies on supercritical fluids, the nonlinear density dependence has been ascribed to the difference between bulk and local density. This is because $\Delta \nu_A$ is linear to density according to the mean field approximation as [39]

$$\Delta \nu_A = C_A \rho \tag{3}$$

where C_A is coefficient depending on solute and solvent molecules. Thus, the nonlinearity as shown in Fig. 4 arises from density inhomogeneity in a real system. LDA enables us to

quantitatively evaluate how much of the density is locally excess relative to the bulk density [40–44] and is defined as

$$(\rho_{local} - \rho)/\rho_c, \quad (4)$$

where ρ_{local} and ρ represent local solvent density around a solute molecule and the averaged solvent density, respectively. The local density is generally estimated by finding the density that gives the same amount of shift on a linear line as it does on a nonlinear curve (Fig. 5a). Based on the equation (4), the LDA was estimated. Figs. 5b and 5c show the LDA of *cis*- and *trans*-DPE, respectively [45,46,48]. It was evaluated that LDA of *trans*-DPE is twice times greater than that of *cis*-DPE. Thus, it is concluded that many solvent molecules can surround the two phenyl groups in *trans*-DPE due to the absence of steric hindrance and significant solvation results in *trans*-DPE.
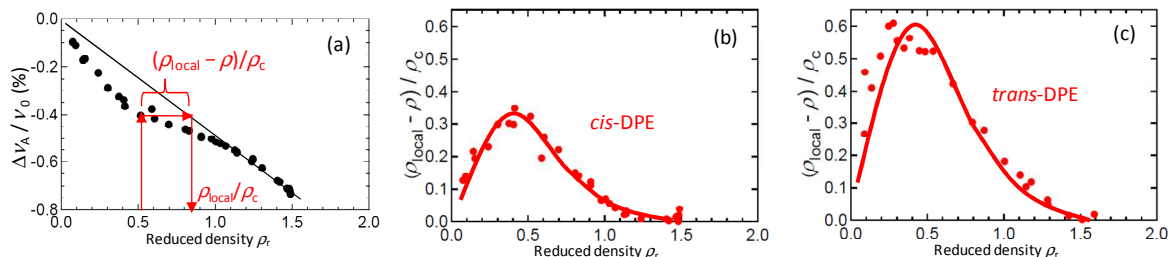

Figure 5. The local density augmentation. (a) The method to obtain the local density augmentation, $(\rho_{local} - \rho)/\rho_c$. Symbols are experimental attractive shifts. Solid line is linear line based on the mean field approximation. (b, c) Local density augmentations of (b) *cis*-DPE and (c) *trans*-DPE in scCO$_2$. The quantity of ρ_r is expressed as $\rho_r = \rho/\rho_c$. Solid lines are visual guides obtained by fitting polynomial functions to the data.

CONCLUSIONS

The Raman spectra of the C=C stretching modes of *cis*-DCE, *cis*-DPE, and *trans*-DPE were measured in scCO$_2$ or scCHF$_3$ along an isotherm of $T_r = 1.02$ over wide range of density of $0.08 < \rho_r < 1.7$. Peak frequency of *trans*-DPE shifted significantly, as the density increased. The shifted amount was 20 times greater than that of *cis*-DCE, and was equivalent to those of typical hydrogen-bonded fluids. The large shift of *trans*-DPE was attributed to a functional group effect of site-selective solvation around a phenyl group in the absence of steric hindrance. For the *trans*-DPE in scCO$_2$, significant LDA was also observed. From these findings, we can conclude that functinal group (phenyl group) and molecular structure (no steric hindrance) produce solvation structure.

REFERENCES

[1] Buckingham, A. D., Proc. Roy. Soc. A, Vol. 248, **1958**, p. 169.

[2] Reichardt, C., *Solvents and Solvent Effects in Organic Chemistry* (Wiley-VCH, Weinheim, **2003**).

[3] *Supercritical Fluids : Molecular Interactions, Physical Properties, and New Applications*, edited by Arai, Y., Sako, T., Takebayashi, Y. (Springer, Berlin, **2002**).

[4] Ben-Amotz, D., LaPlant, F., Shea, D., Gardecki, J., List, D., in *Proceedings of the Supercritical Fluids Technology*, ACS Symposium Series No. 488, edited by Bright, F. V., McNanlly, M. E. (American Chemical Society, Washington, DC, **1993**).

[5] Devendorf, G. S., Ben-Amotz, D., de Souza, L. E. S., J. Chem. Phys., Vol. 104, **1996**, p. 3479.

[6] Pan, X., McDonald, J. C., MacPhail, R. A., J. Chem. Phys., Vol. 110, **1999**, p. 1677.

[7] Saitow, K., Otake, K., Nakayama, H., Ishii, K., Nishikawa, K., Chem. Phys. Lett., Vol. 368, **2003**, p. 209.

[8] Saitow, K., Nakayama, H., Ishii, K., Nishikawa, K., J. Phys. Chem. A, Vol. 108, **2004**, p.5770.

[9] Lalanne, P., Tassaing, T., Danten, Y., Cansell, F., Tucker, S. C., Besnard, M., J. Phys. Chem. A, Vol. 108, **2004**, p. 2617.

[10] Saitow, K., Sasaki, J., J. Chem. Phys., Vol. 122, **2005**, p. 104502.

[11] Tassaing, T., Oparin, R., Danten, Y., Besnard, M., J. Supercrit. Fluids, Vol. 33, **2005**, p. 85.

[12] Cabaco, M. I., Besnard, M., Tassaing, T., Danten, Y., J. Mol. Liq., Vol. 125, **2006**, p. 100.

[13] Kajiya, D., Mouri, Y., Saitow, K., J. Phys. Chem. B, Vol. 112, **2008**, p. 7980.

[14] Kajiya, D., Saitow, K., J. Phys. Chem. B, Vol. 113, **2009**, p. 13291.

[15] Kajiya, D., Saitow, K., J. Phys. Chem. B, Vol. 114, **2010**, p. 8659.

[16] Kajiya, D., Saitow, K., J. Phys. Chem. B, Vol. 114, **2010**, p. 16832.

[17] Osawa, K., Hamamoto, T., Fujisawa, T., Terazima, M., Sato, H., Kimura, Y., J. Phys. Chem. A, Vol. 113, **2009**, p. 3143.

[18] Yui, K., Uchida, H., Itatani, K., Koda, S., Chem. Phys. Lett., Vol. 477, **2009**, p. 85.

[19] Yasaka, Y., Kubo, M., Matubayasi, N., Nakahara, M., Bull. Chem. Soc. Jpn., Vol. 80, **2007**, p. 1764.

[20] Fujisawa, T., Terazima, M., Kimura, Y., J. Phys. Chem. A, Vol. 112, **2008**, p. 5515.

[21] Akimoto, S., Kajimoto, O., Chem. Phys. Lett., Vol. 209, **1993**, p. 263.

[22] Saitow, K., Ochiai, H., Kato, T., Nishikawa, K., J. Chem. Phys. Vol. 116, **2002**, p. 4985.

[23] Saitow, K., Kajiya, D., Nishikawa, K., J. Am. Chem. Soc., Vol. 126, **2004**, p. 423.

[24] Saitow, K., Kajiya, D., Nishikawa, K., J. Phys. Chem. A, Vol. 109, **2005**, p. 83.

[25] Kajiya, D., Nishikawa, K., Saitow, K., J. Phys. Chem. A, Vol. 109, **2005**, p. 7365.

[26] Saitow, K., Nishikawa, K., Ohtake, H., Sarukura, N., Miyagi, H., Shimokawa, Y., Matsuo, H., Tominaga, K., Rev. Sci. Inst., Vol. 71, **2000**, p. 4061.

[27] Saitow, K., Ohtake, H., Sarukura, N., Nishikawa, K., Chem. Phys. Lett., Vol. 341, **2001**, p. 86.

[28] Nakayama, H., Saitow, K., Sakashita, M., Ishii, K., Nishikawa, K., Chem. Phys. Lett., Vol. 320, **2000**, p. 323.

[29] Otake, K., Abe, M., Nishikawa, K., Saitow, K., Jpn. J. Appl. Phys., Vol. 45, **2006**, p. 2801.

[30] Kajiya, D., Saitow, K., J. Chem. Phys., Vol. 134, **2011**, p. 234508.

[31] Saitow, K., J. Phys. Chem. B, Vol. 109, **2005**, p. 3731.

[32] Saitow, K., Yamamura, T., Minami, T., J. Phys. Chem. C, Vol. 112, **2008**, p. 18340.

[33] Saitow, K., Yamamura, T., J. Phys. Chem. C, Vol. 113, **2009**, p. 8465.

[34] Saitow, K., Chapter 12 in *Nanoparticle Generation by Laser Ablation in Liquid and Supercritical Fluid Laser Ablation in Liquid: Principles, Methods, and Applications in Nanomaterials Preparation and Nanostructures Fabrication*, edited by Yang, G. W. (Pan Stanford publishing, Singapore, **2011**).

[35] Span, R., Wagner, W., J. Phys. Chem. Ref. Data, Vol. 25, **1996**, p. 1509.

[36] Penoncello, S. G., Lemmon, E. W., Jacobsen, R. T., Shan, Z., J. Phys. Chem. Ref. Data, Vol. 32, **2003**, p. 1473.

[37] Zakin, M. R., Herschbach, D. R., J. Chem. Phys., Vol. 85, **1986**, p. 2376.

[38] Favero, F. W., Skaf, M. S., J. Supercrit. fluids, Vol. 34, **2005**, p. 237.

[39] Schweizer, K. S., Chandler, D., J. Chem. Phys., Vol. 76, **1982**, p. 2296.

[40] Song, W., Maroncelli, M., Chem. Phys. Lett., Vol. 378, **2003**, p. 410.

[41] Nugent, S., Ladanyi, B. M., J. Chem. Phys., Vol. 120, **2004**, p. 874.

[42] Skarmoutsos, I., Dellis, D., Samios, J., J. Phys. Chem. B, Vol. 113, **2009**, p. 2783.

[43] Skarmoutsos, I., Guàrdia, E., J. Phys. Chem. B, Vol. 113, **2009**, p. 8887.

[44] The increase of local solvent density around solute has been expressed by augmentation, enhancement, excess, and clustering. In the present paper, we use the local density augmentation, defined in references 40-44.

[45] The LDA causes $\Delta \nu_R$ and $\Delta \nu_A$ to increase. Thus, we examined how amount $\Delta \nu_R$ and $\Delta \nu_A$ are changed using local density. The calculation was performed at $\rho_r = 0.5$, at which local density augmentation reaches a maximum. The increases in $\Delta \nu_R$ and $\Delta \nu_A$ by the local density augmentation were lower than 0.09%.

[46] LDA around benzene in $scCO_2$ was investigated by infrared spectroscopy in reference 47 and it was estimated that the value of LDA is about 0.45 at $\rho_r = 0.5$, which value is 1.3 times smaller than that around *trans*-DPE.

[47] Wada, N., Saito, M., Kitada, D., Smith, Jr., R. T., Inomata, H., Arai, K., Saito, S., J. Phys. Chem B, Vol. 101, **1997**, p. 10918.

[48] We confirmed that the density dependence of LDA in $scCO_2$ is the same as that in $scCHF_3$.